AIAA JOURNAL
Vol. 41, No. 8, August 2003

Correlating Friction Velocity in Turbulent Boundary Layers Subjected to Freestream Turbulence

Michael J. Barrett*
Valparaiso University, Valparaiso, Indiana 46383
and
D. Keith Hollingsworth†
University of Houston, Houston, Texas 77204

A turbulent boundary layer was subjected to grid-generated freestream turbulence to study the effects of turbulent length scale and intensity on skin friction. The study emphasized the importance of the turbulent-to-viscous length scale ratio and focused on correlating skin friction without the use of conventional boundary-layer Reynolds numbers. The experimental data were characterized by small-scale freestream turbulence above boundary layers with momentum-thickness Reynolds numbers ranging from 225 to 2700. Freestream turbulence intensities varied from 0.1 to 8.0%. The turbulent-to-viscous length scale ratios spanned from 100 to 1000, and ratios of freestream turbulent length scale to boundary-layer momentum thickness ranged from 4 to 32. A new boundary-layer model was used to establish a skin-friction correlation that does not require knowledge of the momentum-thickness Reynolds number. The correlation was evaluated using the new small-scale data and other data from the literature. When only freestream information (length scale, mean velocity, and turbulence intensity) was employed, the correlation provided an estimate of the friction velocity to within 8% (20:1 odds). The correlation was evaluated using data with momentum-thickness Reynolds numbers up to 6300, freestream intensities as large as 29%, turbulent-to-viscous length scales reaching 11,000, and length scale-to-boundary-layer momentum-thickness values as high as 190.

Nomenclature

C_f	=	skin-friction coefficient, $2\tau_w/\rho u_\infty^2$ or $2u_\tau^2/u_\infty^2$
L	=	turbulent length scale
l	=	sensor wire length
Re	=	Reynolds number
Tu	=	turbulence intensity, $u'/\bar{u}$
u	=	streamwise velocity
u_τ	=	boundary-layer friction velocity, $\sqrt{(\tau_w/\rho)}$
v	=	velocity in direction normal to surface
x	=	streamwise coordinate
y	=	coordinate in direction normal to the surface
δ	=	boundary-layer thickness
θ	=	boundary-layer momentum thickness
ν	=	kinematic viscosity
σ	=	standard deviation
τ_w	=	wall shear stress

Subscripts

e	=	energy based
w	=	wall
0	=	at the same Re_θ in a $Tu_\infty = 0$ flow
15	=	located at $y^+ = 15$
∞	=	freestream

Superscripts

–	=	Reynolds averaged mean
$'$	=	fluctuating (rms value)
$+$	=	nondimensionalized using wall variables

Received 3 August 2002; revision received 24 January 2003; accepted for publication 30 January 2003.

*Assistant Professor, Mechanical Engineering Department. Senior Member AIAA.
†Associate Professor, Department of Mechanical Engineering.

Introduction

DESIGN engineers daily encounter difficulty in accurately predicting skin friction for turbulent boundary layers subjected to freestream turbulence (FST). Existing correlations and numerical techniques are still limited by a priori information requirements and the raw computational complexity of flows with moderate to high Reynolds numbers. To aid the design engineer, this work establishes a friction–velocity correlation that uses only freestream information. The hope is to develop a useful correlation that relies on only a few readily estimated input parameters.

We begin with a summary of earlier FST work that developed techniques to correlate skin friction. In the context of the earlier works, we present the objectives of the current study. The experimental methods used to gather new small-scale data are briefly described. Baseline experimental results are displayed to validate the investigative techniques. Data for the elevated FST cases are given; we showcase the very small freestream length scales achieved. With use of new data, earlier correlation methods are evaluated. Following the evaluation, we develop a new friction–velocity correlation that does not need momentum-thickness Reynolds number as input. From the results, we draw conclusions that address the stated experimental objectives.

Literature Review

Simonich and Bradshaw[1] initiated one of the modern approaches to evaluating FST effects on flat-plate boundary-layer skin friction. They examined the effects of varying Tu_∞ and L/δ. (The length L roughly scales with the size of the energy-containing turbulent eddies.) They showed that C_f increased as Tu_∞ increased and L/δ decreased. Their work also extended the Kader and Yaglom[2] scaling analysis. Simonich and Bradshaw[1] noted the viscous length scale, ν/u_τ, was the compatible reference length for the similarity analysis. However, they used θ because it was more convenient to compare boundary layers at similar Reynolds number Re_θ values. The use of Re_θ was an improvement over Re_x comparisons; however, it diluted the importance of $L/(\nu/u_\tau)$ similarity.

Hancock and Bradshaw[3] conducted the first systematic evaluation of the effect of L_∞ on boundary-layer skin friction. They presented

the enhancement proportionality,

$$\Delta C_f / C_{f_0} \propto Tu_\infty/(2 + L/\delta) \tag{1}$$

The grouping $Tu_\infty/(2 + L/\delta)$ is termed the Hancock–Bradshaw (HB) parameter.

Blair[4,5] examined C_f using the HB parameter. With low Re_θ data, Blair added a "damping-term,"

$$\mathrm{HB}_{\mathrm{mod}} = Tu_\infty/\{(2 + L/\delta)[1 + 3\exp(-Re_\theta/400)]\} \tag{2}$$

He concluded that $\Delta C_f/C_{f_0}$ was proportional to $\mathrm{HB}_{\mathrm{mod}}$. Whereas others offered similar modifications (for example, Castro[6]), we use $\mathrm{HB}_{\mathrm{mod}}$ given in Eq. (2) to represent this type of analysis.

In discussing Tu_∞ effects on boundary-layer structure, Hancock and Bradshaw[7] showed that wake strength and other integral parameters also correlated with HB.

Johnson and Johnston[8] recorded some of the smallest L/δ to date; they used a passive biplanar grid in a water tunnel. Their Tu_∞ ranged from 4.7 to 7.5%; the L/δ ratios varied from 0.27 to 0.4. For Re_θ variation from 1150 to 1475, they showed $\Delta C_f/C_{f_0}$ of 15–18%.

Ames and Moffat[9] studied large-scale, high Tu_∞ effects. They used results from Hunt and Graham[10] to introduce correlations for C_f enhancement. They obtained

$$\Delta C_f/C_{f_0} \propto Tu_\infty(\theta/L)^{\frac{1}{3}}(Re_\theta/1000)^{\frac{1}{4}} \tag{3}$$

where the right-hand side of Eq. (3) is called TLR_m.

Sahm and Moffat[11] examined FST effects in flows with curvature; however, they also provided some flat-plate results. Using passive and jet grids, they examined flows with Tu_∞ as high as 29%. Their data suggested the freestream was not fully developed in the flat-plate region behind the grid. As they noted, the flat-plate boundary layer thinned as it progressed downstream.

Hollingsworth and Bourgogne[12] examined momentum boundary layers growing under a fully turbulent shear layer. Despite stress-driven three dimensionality in the resultant flow, they found that two-dimensional scaling laws applied in the boundary layer near-wall and inner-core regions. These observations were affirmed in the heat transfer study of Maniam and Hollingsworth.[13]

Thole[14] and Thole and Bogard[15,16] studied Tu_∞ effects using wall-injection jets. Their work reaffirmed boundary-layer flux correlation with HB and TLR. From the heat-transfer work of Maciejewski and Moffat,[17,18] Thole[14] and Thole and Bogard[15,16] derived a skin-friction coefficient based on a near-wall fluctuating velocity, C'_f. They showed that C'_f varies with Tu_∞; they observed no L_∞ or Re dependence.

Bott and Bradshaw[19,20] used a passive grid in a wind tunnel with a rotating belt as the wall. When belt speed was varied, their Tu_∞ values [calculated as $u'_\infty/(\bar{u}_\infty - \bar{u}_w)$] were larger than those in earlier passive-grid studies. Enhancements were presented in terms of $\mathrm{HB}_{\mathrm{mod}}$ and the Castro[6] parameter.

Finally, three other studies are useful as contextual references. Camp and Shin[21] observed compressor-blade wakes coherently propagating into downstream blade passages; the wakes produced passage-flow L_∞ values as small as 4% of mean chord. Ames and Plesniak[22] (also Ames[23]) recorded L_∞/θ as low as 9.5 in an apparatus representing the first stator row after the exit of a combustor. Even though wakes from upstream blades were absent, scales in the blade passage were significantly smaller than those generated by the combustor. Blade-passage Tu_∞ values measured between 2 and 3%; Re_θ varied from 2400 to 2600. Halstead et al.[24] provided extensive measurements from a rotating, multistage turbine test apparatus. Peak Tu_∞ values in downstream stages coincided with the passing of coherent wakes from upstream blades. The likely small-scaled wakes carried peak intensities of less than 5%. Suction-surface Re_θ values ranged from 100 to 1000; the highest values were measured during engine startup conditions.

Present Objectives

We have identified two existing methods to account for FST effects. The first uses FST characteristics to correlate $\Delta C_f/C_{f_0}$. The HB and TLR methods are both of this type. The second makes use of a near-wall skin-friction coefficient C'_f assumed to be only a function of Tu_∞. The requisite Re_θ or u' information restrict the predictive usefulness of either method.

Framed in this context, we adopt three objectives for the present work: 1) for Re_θ and Tu_∞ representative of flows in aircraft turbines, investigate the effect of small-scale FST on C_f, 2) closely examine the possibility of length scale dependence in C'_f, and 3) for elevated Tu_∞, correlate $u_\tau/\bar{u}_\infty$ to the FST without reference to Re_θ.

Experimental Methods

Velocities were measured using hot-wire anemometers in flat-plate air boundary layers subjected to grid-generated turbulence. Both single- and two-wire probes were used to examine turbulence characteristics; however, the new skin-friction and velocity data used in developing the correlation are based on single-wire measurements only. The single-wire probe was 0.5 mm long with a 2.5-μm diameter. The dimensionless sensor length l^+ ranged from 3 to 15, and the sensor length never exceeded 4% of the measured integral length scale L_e. For measurements at $y^+ = 15$, the ratio formed by dividing y by the wire radius fell below 500 only twice (392 and 461). Near-wall conduction effects are expected to be negligible for ratios greater than 500 (Ref. 25); no corrections were made to the raw data to account for this phenomenon. The u' fluctuation wire-length correction of Maniam[26] was used for the $y^+ = 15$ data only. (Profiles were not adjusted.) The correction was small (2–8%) and did not affect the overall results, particularly because the correlation development included many other data sets from studies using different measurement methods. Conventional measurement techniques were used in the current study and are reported elsewhere[27–30]; see the earlier works for additional details.

Experimental Results

Clean Freestream (CFS) Validation Data

Figure 1 shows u^+ profiles measured at different Re_θ and compares them with the near-wall and logarithmic profiles given by Kays and Crawford[31]:

$$u^+ = y^+ \qquad \text{for} \qquad y^+ < 5 \tag{4}$$

$$u^+ = 2.44\,\ell n(y^+) + 5.0 \qquad \text{for} \qquad 50 < y^+ < \text{wake} \tag{5}$$

The direct numerical simulation (DNS) results of Spalart[32] are also presented for comparison. Even the $Re_\theta \cong 500$ profile still exhibits a small logarithmic region. Figure 2 shows profiles of u'^+. At similar Re_θ, the data generally compare well with Spalart's results.

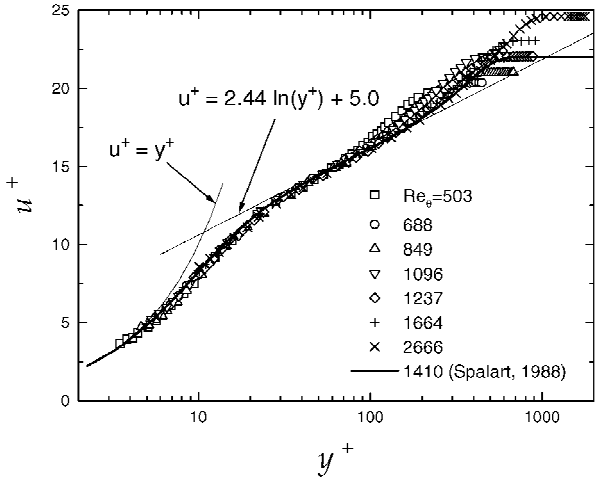

Fig. 1 CFS mean velocity profiles.

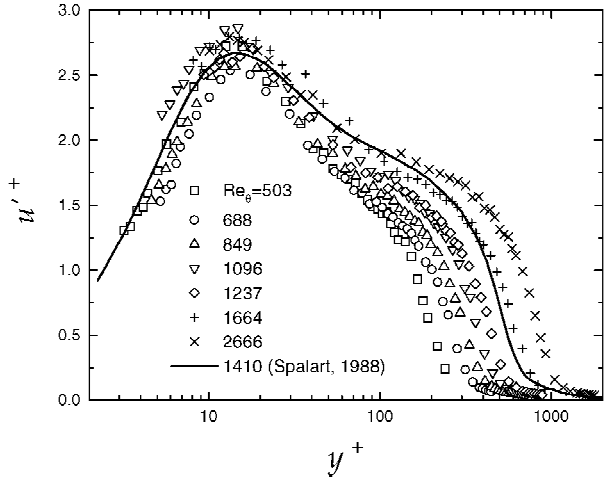

Fig. 2 CFS streamwise fluctuation profiles.

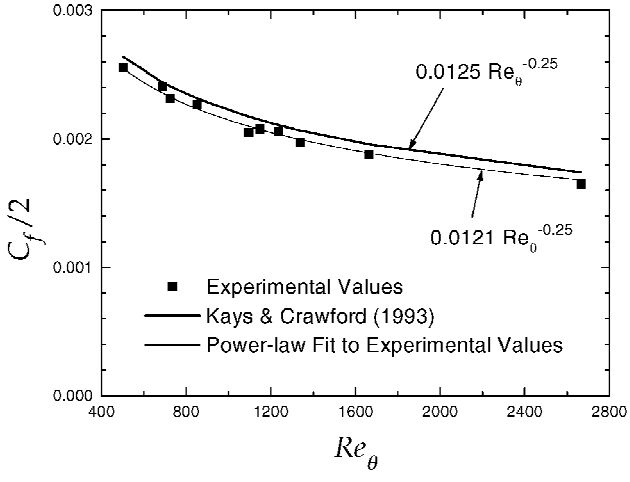

Fig. 3 CFS skin-friction coefficient vs Re_θ.

Figure 3 shows $C_f/2$ plotted vs Re_θ and the correlation of Kays and Crawford,[31]

$$C_f/2 = 0.0125\, Re_\theta^{-\frac{1}{4}} \tag{6}$$

The current values lie slightly below the correlation, but they are within the typical experimental uncertainty of ±5% on C_f for clean freestream (CFS) flows.

Turbulent Length Scales

Most of the previous studies examined flows with $L_{e,\infty}$ that are much larger than the turbulence scales in the inner region of the boundary layer and often much larger than the scales in the boundary-layer core. However, much of the current data represent flows with $L_{e,\infty}$ smaller than scales in the boundary-layer core, and some profiles have $L_{e,\infty}$ as small as scales in the log region. To illustrate, two boundary-layer profiles of L_e^+ (L_e divided by ν/u_τ) are shown in Fig. 4. In both cases, the outer region is seeded with scales smaller than those that would naturally occur from shear-produced turbulence; for both profiles, $L_{e,\infty}$ is smaller than the mean-velocity-based boundary-layer thickness. However, for the filled symbols, L_e decreases from the freestream value as we traverse the core and approach the wall. The open symbols show a boundary layer with a more unusual scale distribution: The L_e introduced from the freestream are as small as those in the log region.

Figure 5 shows a comparison of θ/L_e values in the current work to previous studies. Length scales were measured at $y^+ = 150$ for the CFS case. The current investigation examines $L_{e,\infty}$ as small (relative to θ) as those obtained by Johnson and Johnston[8] and an order of magnitude smaller than many studies. In comparison to

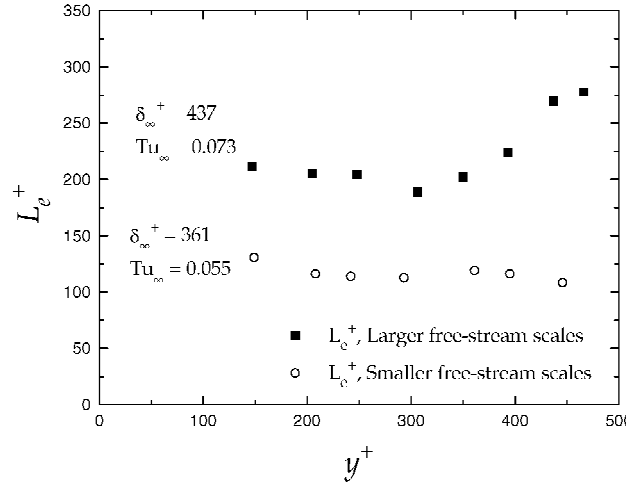

Fig. 4 L_e^+ length scale profiles.

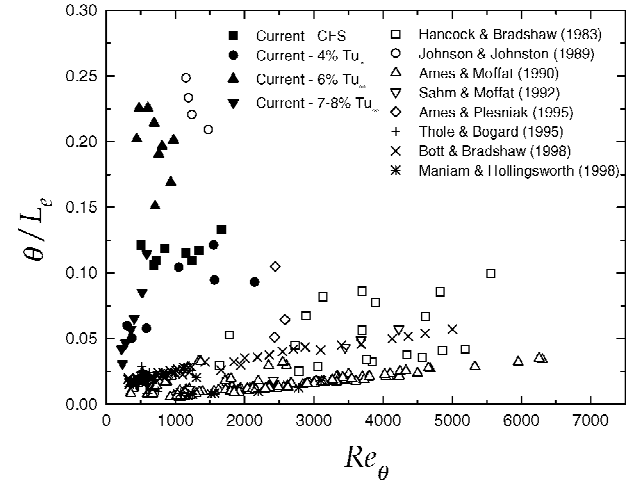

Fig. 5 Length scale ratios in current and previous studies (θ/L_e vs Re_θ).

the viscous length scale, ν/u_τ, Fig. 6 shows that the current scales are the smallest examined. Figure 5 also exhibits the Tu_∞ and Re_θ ranges of the current study. The ranges cover those applicable to multistage low-pressure gas turbines as identified by Halstead et al.[24] Worst-case experimental uncertainties for Tu_∞ and Re_θ were 3.5 and 7%, respectively.

Boundary-Layer Response to FST

Typical velocity profiles with FST are given in Fig. 7. For comparison to the CFS validation cases, the DNS results of Spalart[32] are shown. The mean profile shows strong agreement with the DNS through the buffer layer and a portion of the log layer.

Measured C_f are shown in Fig. 8. When compared to Eq. (6), the CFS Re_θ-based correlation, enhancements between 6 and 16% are observed in the present data.

Analysis of Results

Established Skin-Friction Comparisons

Figure 9 shows measured C_f enhancements in terms of HB_{mod}. To facilitate consistency and to accurately represent the correlative scatter a design engineer might encounter, Eq. (6) is used as the CFS reference for all data sets; actual C_f values were compared to those predicted using Eq. (6) without adjustment for a specific experimental apparatus. The HB_{mod} parameter collects $\Delta C_f/C_{f0}$ to within about ±40%. When the functional dependence indicated by the solid line in Fig. 9 is used, a variation of ±4% (±2σ of data shown) is found for $(C_f/2)^{1/2}$ predictions using the HB_{mod} parameter; direct $(C_f/2)^{1/2}$ results are shown in Fig. 10. [We choose to

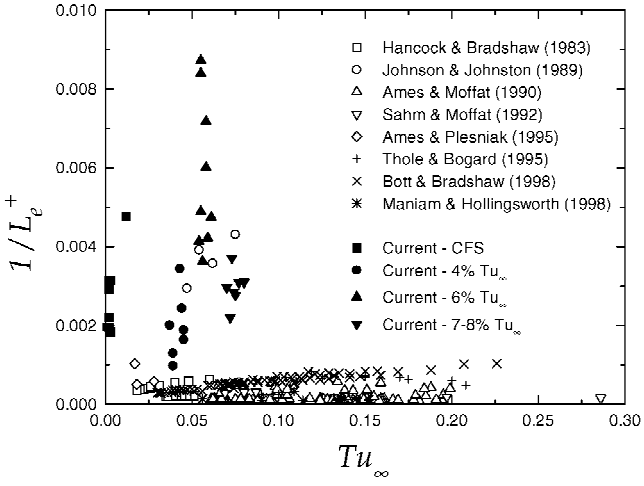

Fig. 6 Length scale ratios in current and previous studies ($1/L_e^+$ vs Tu_∞).

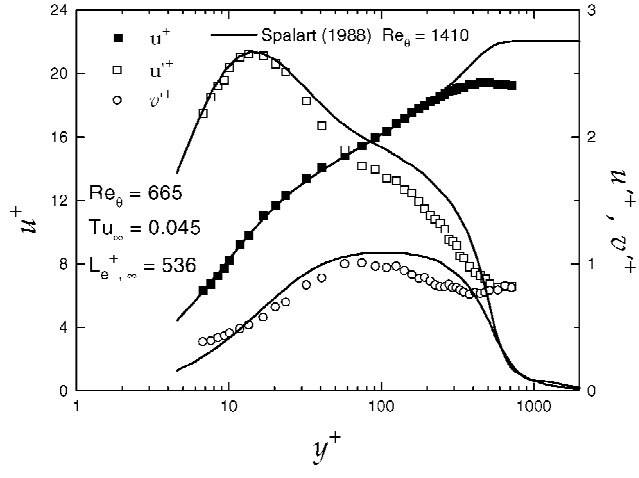

Fig. 7 Dimensionless velocity profiles with elevated Tu_∞.

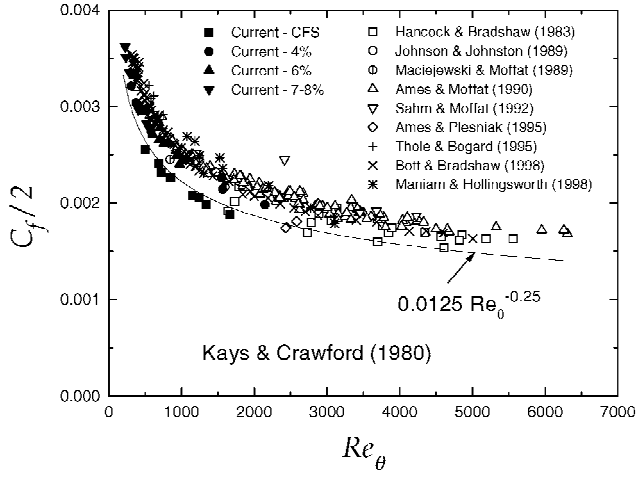

Fig. 8 Skin-friction coefficient vs Re_θ.

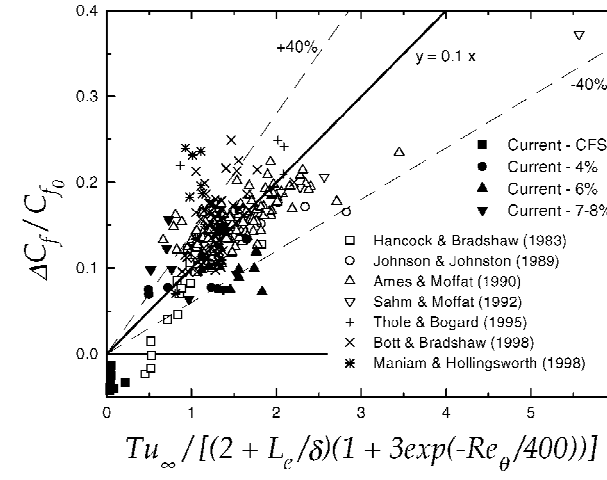

Fig. 9 C_f enhancement vs modified HB.

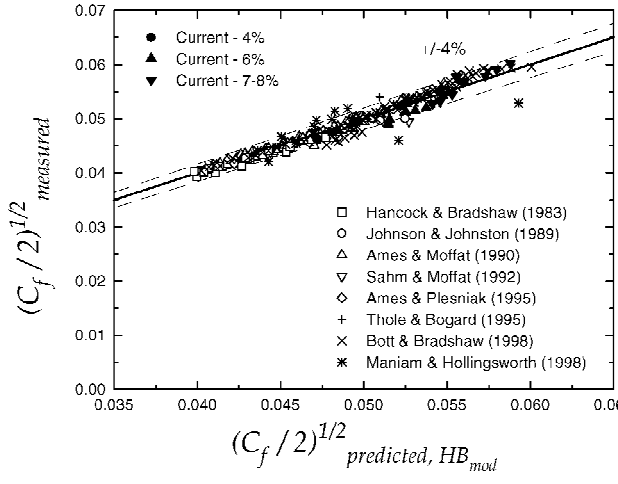

Fig. 10 Measured C_f vs predicted C_f using modified HB.

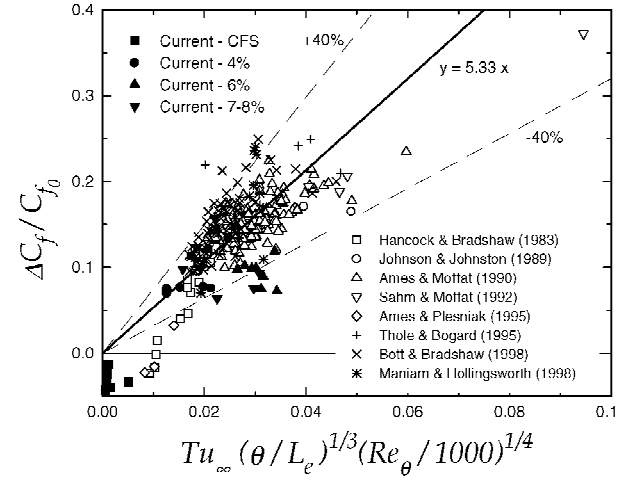

Fig. 11 C_f enhancement vs TLR_m.

display the data as $(C_f/2)^{1/2}$, that is, $u_\tau/\bar{u}_\infty$, because this velocity ratio can be used to correlate heat transfer using only freestream parameters.[30,33]] Figure 11 shows that TLR_m behaves similarly when examining C_f enhancement. Presented in Fig. 12, TLR_m yields direct $(C_f/2)^{1/2}$ predictions to within ±3%. The collapse of data using these two Re_θ-based correlations is quite remarkable when one considers that first-order experimental uncertainty in C_f typically ranges from ±3 to ±6%. The equivalent first-order uncertainty in $(C_f/2)^{1/2}$ of ±1.5% to ±3% leaves little for nth-order effects.

Thole and Bogard[15] observed variation in the value of C_f' due to its dependence on Tu_∞. Combining the current small-scale data with earlier observations in Fig. 13, an explicit dependence on $L_{e,\infty}$ is now also apparent. Over the length scale range shown, the value of C_f' drops approximately 50%. A log–linear regression analysis yields odds of less than 1:10^{19} ($p < 10^{-19}$) that C_f' and L_e^+ are not correlated.

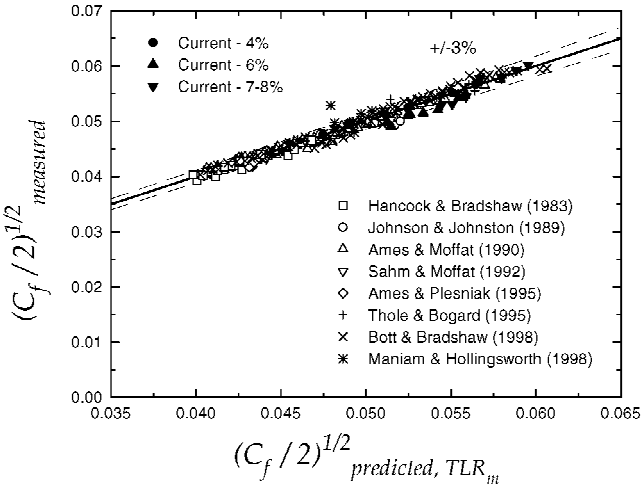

Fig. 12 Measured C_f vs predicted C_f using TLR$_m$.

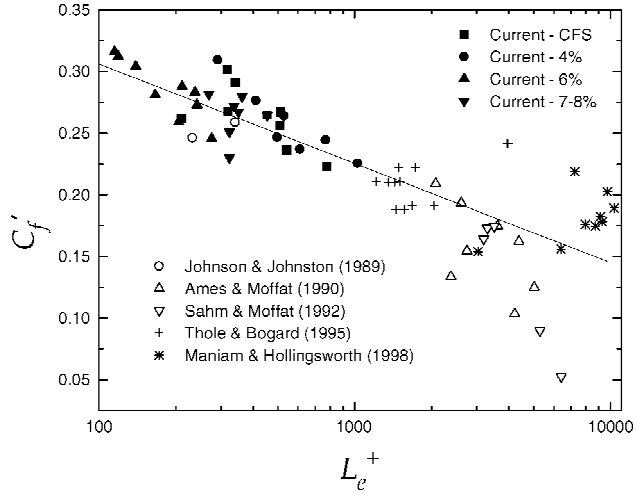

Fig. 13 C_f' dependence on length scale.

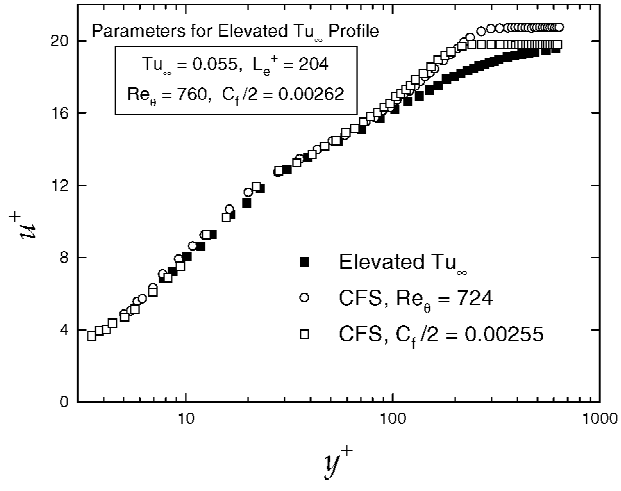

Fig. 14 Elevated Tu_∞ and CFS profile comparison.

Development of C_f Correlation

When the effect of FST is characterized in terms of $\Delta C_f/C_{f_0}$, the need for advance knowledge of Re_θ limits the predictive usefulness of the correlation. Our data indicate, as other investigators have shown, that, when streamwise pressure gradients are small, the u^+ profile in the sublayer and the buffer layer is largely unchanged regardless of Tu_∞. Often, a significant portion of the log-layer also follows Eq. (5). To develop a C_f correlation that does not require Re_θ information, we begin by examining the two-dimensional boundary-layer momentum equation and the implications of a universal u^+ profile in the sublayer and buffer layer. The two-dimensional Reynolds averaged x-momentum equation for an incompressible Newtonian fluid with negligible bulk viscosity and constant properties is given by

$$\bar{u}\frac{\partial \bar{u}}{\partial x} + \bar{v}\frac{\partial \bar{u}}{\partial y} = \frac{\partial}{\partial y}\left(\nu\frac{\partial \bar{u}}{\partial y} - \overline{u'v'}\right) \tag{7}$$

Equation (7) assumes the body forces and streamwise pressure gradient are negligible. Making the equation dimensionless using wall variables, we write

$$u^+\frac{\nu}{u_\tau^2}\frac{\partial \bar{u}}{\partial x} + v^+\frac{\partial u^+}{\partial y^+} = \frac{\partial}{\partial y^+}\left(\frac{\partial u^+}{\partial y^+} - uv^+\right) \tag{8}$$

When the incompressible continuity equation is employed, Eq. (8) can be written

$$-u^+\frac{\partial v^+}{\partial y^+} + v^+\frac{\partial u^+}{\partial y^+} = \frac{\partial}{\partial y^+}\left(\frac{\partial u^+}{\partial y^+} - uv^+\right) \tag{9}$$

We temporarily focus on only the sublayer and buffer layer; let us assume that $u^+ = u^+\{y^+\}$ is universal as the data[34] suggest. Equation (9) then directly governs the relationship between v^+ and uv^+ near the wall. If v^+ were dependent on y^+ only, then Eq. (9) would be an ordinary differential equation with y^+ as the independent variable. For an impenetrable surface, the inner boundary conditions for u^+, v^+, and uv^+ all equal zero. Although there are still two dependent variables in the equation and we recognize that the solution is not unique, Eq. (9) demonstrates that near-wall behavior is tightly restricted by the value of uv^+ at the buffer-layer outer boundary (the inner edge of the boundary-layer core). Additional constraints related to likely monotonic behaviors in this region further limit the set of possible solutions. This entire approach suggests that viewing the mean velocity profile in terms of a near-wall and a core region may prove useful.

Focus again on the entire boundary layer: Figure 14 shows three u^+ profiles. One profile is for a flow with FST; the other two are CFS profiles, one at nearly the same Re_θ and one with nearly the same C_f as that for the FST case. The like-Re_θ profiles have little in common outside a y^+ value of 100. The like-C_f profiles, however, also share outer boundary conditions for $u^+[u_\infty^+ = (C_f/2)^{-1/2}]$ and $uv^+(uv^+_{\infty,\mathrm{CFS}} = 0$ and $uv^+_{\infty,\mathrm{isotropic\ FST}} = 0)$.

The desire to obtain similar outer boundary conditions dictates that we compare profiles with similar C_f values. Recalling that Eq. (9) governs both of these flows and expecting that momentum transport in the core of the boundary layer is dominated by the turbulent component, we propose that the differences in the like-C_f profiles are due primarily to the characteristics of the turbulence in the boundary-layer core. If a gradient-diffusion model that characterizes the diffusivity using a single velocity and length scale can effectively represent the turbulent transport in the core, this proposal leads to the functional statement

$$C_f = C_f\{\boldsymbol{V}, \boldsymbol{L}\} \tag{10}$$

where $\boldsymbol{V}$ and $\boldsymbol{L}$ are the respective characteristic velocity and length scales. We now develop a C_f correlation in accord with this result.

Maniam and Hollingsworth[13] found that, for the CFS turbulent boundary layer,

$$u'_{15}/u_\tau = 2.06\,Re_\theta^{1/24} \tag{11}$$

Using CFS data taken at $y^+ = 150$, Barrett[29] developed the relationship

$$L_e^+ = 2.25\, Re_\theta^{\frac{3}{4}} \tag{12}$$

relating L_e^+ in the core of the boundary layer to Re_θ. Combining Eqs. (11) and (12), we write

$$u'_{15}/u_\tau = 1.97\left(L_e^+\right)^{1/18} \tag{13}$$

Figure 15 shows a comparison of Eq. (13) with data from this and other studies regardless of FST level. Freestream values were used for L_e in all cases with FST; values at $y^+ = 150$ were used for the CFS cases. When it is considered that Eq. (13) was derived using only CFS information, except for one high Tu_∞ case of Sahm and Moffat,[11] the data in Fig. 15 are encouraging.

We develop the correlation by first writing

$$\sqrt{C_f/2} = u_\tau/\bar{u}_\infty = (u_\tau/u'_{15})(u'_{15}/u'_\infty)(u'_\infty/\bar{u}_\infty) \tag{14}$$

and then rewriting using Eq. (13) and the definition of Tu_∞:

$$\sqrt{C_f/2} = (1/1.97)\left(L_e^+\right)^{-1/18}(u'_{15}/u'_\infty)Tu_\infty \tag{15}$$

We search for a single dimensionless velocity and length scale combination to correlate C_f. If u'_{15}/u'_∞ is solely a function of Tu_∞ and L_e^+, then these two scales will satisfy our criteria. A set of u'^+ profiles is shown in Fig. 16. Note the relationship between u'^+_{15}, u'^+_∞, and Tu_∞. The potential of an identifiable relationship based on this observation motivates our examination of the functional dependence between u'_{15}/u'_∞ and Tu_∞. To extract data from studies that did not measure u'_{15}, we chose to calculate the u'_{15}/u'_∞ value by rearranging Eq. (15):

$$u'_{15}/u'_\infty = 1.97\sqrt{C_f/2}\left(L_e^+\right)^{1/18}/Tu_\infty \tag{16}$$

The result using nine data sets is shown in Fig. 17. For consistency, Eq. (16) was used to analyze the data from each study. Despite the wide range of flow conditions represented, all of the data in Fig. 17 are well represented by the power law fit given by

$$u'_{15}/u'_\infty = 0.231\, Tu_\infty^{-0.82} \tag{17}$$

We now combine Eqs. (15) and (17) to arrive at the C_f correlation

$$\sqrt{C_f/2} = TL^+ \tag{18}$$

where TL^+ is defined by

$$TL^+ \equiv 0.117\left(L_e^+\right)^{-1/18} Tu_\infty^{0.18} \tag{19}$$

Figure 18 shows a comparison of Eq. (18) with the data from numerous authors. For a $u_\tau/\bar{u}_\infty$ prediction in terms of only Tu_∞ and $L^+_{e,\infty}$ (not Re_θ), the agreement is again encouraging. Equation (18) provides $(C_f/2)^{1/2}$ predictions to within $\pm 8\%$ ($\pm 2\sigma$ of data shown). The data shown in Fig. 18 cover Tu_∞ from 2 to 30%, L_e^+ from 100 to 11,000, and Re_θ from 300 to 6300. To predict $(C_f/2)^{1/2}$ using Eq. (18), we need know only

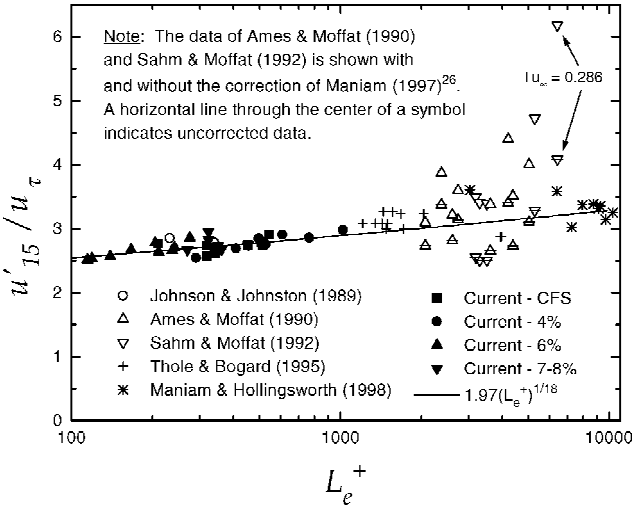

Fig. 15 Near-wall fluctuation vs length scale.

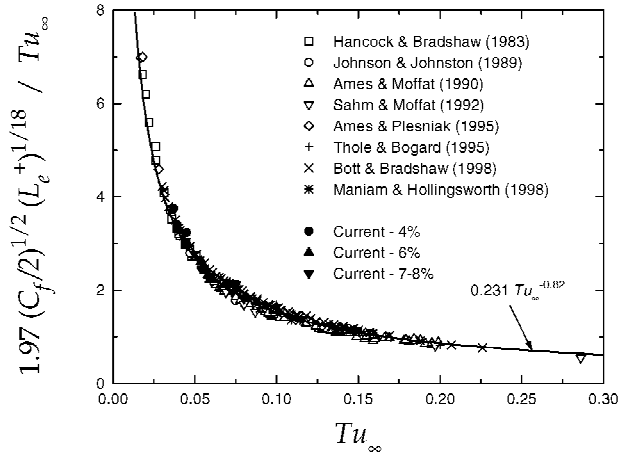

Fig. 17 Velocity-ratio relationship to Tu_∞.

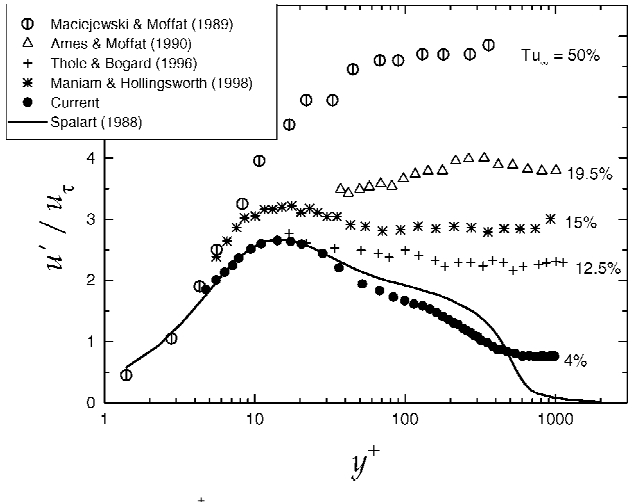

Fig. 16 Profiles of u'^+ from various studies at different levels of Tu_∞.

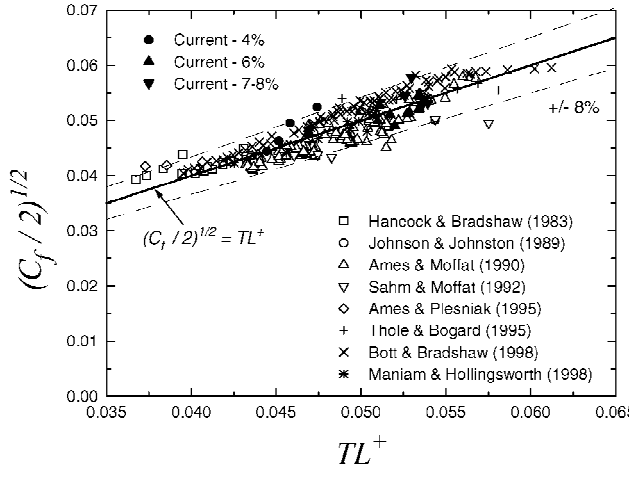

Fig. 18 Dimensionless friction velocity correlated using TL^+.

Table 1 Summary of scatter and input information for the various correlations

Parameter	HB_{mod}	TLR_m	TL^+ [Eq. (19)]
$\pm 2\sigma$ Departure on $(C_f/2)^{1/2}$, %	4	3	8
Tu_∞	Required	Required	Required
$L_{e,\infty}$	Required	Required	Required
$\bar{u}_\infty$	Required	Required	Required
θ	Required	Required	

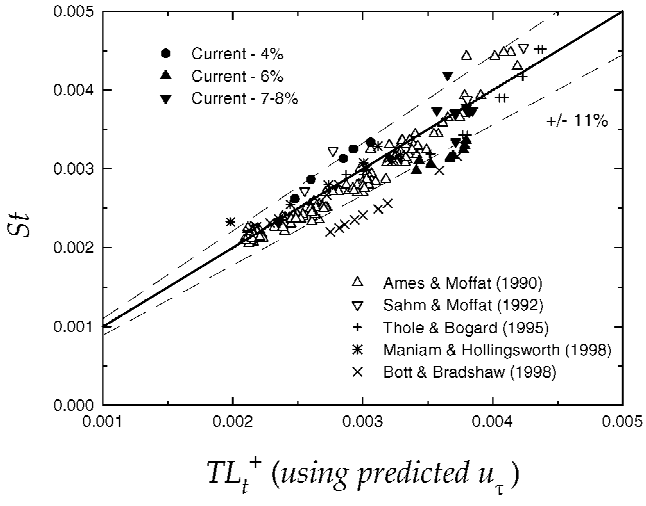

Fig. 19 Heat transfer correlation using Eq. (18).

$\bar{u}_\infty$, u'_∞, $L_{e,\infty}$, and the fluid properties. When these parameters are used, the unknown in the equation, u_τ, is determined and C_f is calculated.

To evaluate its performance, we compare TL^+ to earlier correlations. Table 1 summarizes the scatter and information requirements for the aforementioned methods. When scatter of $\pm 8\%$ is accepted, Eq. (18) enables a heat transfer correlation[30,33] (also using only freestream information) to capture Stanton number St to within $\pm 11\%$. Data illustrating this correlation are shown in Fig. 19.

Conclusions

Very small-scale, moderate-intensity FST enhances turbulent boundary-layer skin friction up to 16% higher than that predicted using an accepted CFS Reynolds number-based correlation. The HB_{mod} and TLR_m elevated-turbulence correlations adequately capture the small-scale data set.

The C'_f coefficient correlates with freestream length scale. Over the length scale range examined, C'_f drops approximately 50%. A log–linear regression analysis confirms that C'_f and L_e are strongly correlated ($p < 10^{-19}$). The new small-scale data make this observation possible.

For flat-plate turbulent boundary layers subjected to FST, the new TL^+ correlation is able to predict the dimensionless friction velocity using only freestream information. Combining the freestream length scale with mean and fluctuating freestream velocities provides enough information to estimate the dimensionless friction velocity to within $\pm 8\%$. The ratio of turbulent-length-scale-to-viscous-length-scale L_e^+ is used as the characteristic dimensionless length scale.

The new TL^+ correlation compares moderately well in accuracy to earlier correlation methods. The 8% uncertainty band for the new correlation is roughly twice as large as the earlier correlations; however, both HB_{mod} and TLR_m require a priori knowledge of momentum-thickness Reynolds number. Because the TL^+ method does not require Re_θ information, over a convincingly large range of flow conditions, the new correlation is a viable predictive tool. Modifications to include pressure gradient, curvature, and other complicating effects should be pursued.

Acknowledgments

Support was received from the Texas Higher Education Coordinating Board (ATP Grant 003652-944), the University of Houston (UH) Institute for Space Systems Operations, and the UH Energy Laboratory. M. J. Barrett received support from the NASA/Texas Space Grant Consortium and the Society of Automotive Engineers Doctoral Scholars Program. We thank S. J. Kleis for consultation and the use of his wind-tunnel facility.

References

[1]Simonich, J. C., and Bradshaw, P., "Effect of Free-Stream Turbulence on Heat Transfer Through a Turbulent Boundary Layer," *Journal of Heat Transfer*, Vol. 100, 1978, pp. 671–677.

[2]Kader, B. A., and Yaglom, A. M., "Heat and Mass Transfer Laws for Fully Turbulent Wall Flows," *International Journal of Heat and Mass Transfer*, Vol. 15, 1972, p. 2329.

[3]Hancock, P. E., and Bradshaw, P., "The Effect of Free-Stream Turbulence on Turbulent Boundary Layers," *Journal of Fluids Engineering*, Vol. 105, 1983, pp. 284–289.

[4]Blair, M. F., "Influence of Free-stream Turbulence on Turbulent Boundary Layer Heat Transfer and Mean Profile Development, Part I: Experimental Data," *Journal of Heat Transfer*, Vol. 105, 1983, pp. 33–40.

[5]Blair, M. F., "Influence of Free-Stream Turbulence on Turbulent Boundary Layer Heat Transfer and Mean Profile Development, Part II: Analysis," *Journal of Heat Transfer*, Vol. 105, 1983, pp. 41–47.

[6]Castro, I. P., "Effect of Free Stream Turbulence on Low Reynolds Number Boundary Layers," *Journal of Fluids Engineering*, Vol. 106, 1984, pp. 298–306.

[7]Hancock, P. E., and Bradshaw, P., "Turbulence Structure of a Boundary Layer Beneath a Turbulent Free Stream," *Journal of Fluid Mechanics*, Vol. 205, 1989, pp. 45–76.

[8]Johnson, P. L., and Johnston, J. P., "The Effects of Grid-Generated Turbulence on Flat and Concave Turbulent Boundary Layers," Mechanical Engineering Dept., Rept. MD-53, Stanford Univ., Stanford, CA, 1989.

[9]Ames, F. E., and Moffat, R. J., "Heat Transfer with High Intensity, Large Scale Turbulence: The Flat Plate Turbulent Boundary Layer and the Cylindrical Stagnation Point," Mechanical Engineering Dept., Rept. HMT-44, Stanford Univ., Stanford, CA, 1990.

[10]Hunt, J. C. R., and Graham, J. M. R., "Free-Stream Turbulence near Plane Boundaries," *Journal of Fluid Mechanics*, Vol. 84, No. 2, 1978, pp. 209–235.

[11]Sahm, M. K., and Moffat, R. J., "Turbulent Boundary Layers with High Turbulence: Experimental Heat Transfer and Structure on Flat and Convex Walls," Mechanical Engineering Dept., Rept. HMT-45, Stanford Univ., Stanford, CA, 1992.

[12]Hollingsworth, D. K., and Bourgogne, H.-A., "The Development of a Turbulent Boundary Layer in High Free-Stream Turbulence Produced by a Two-Stream Mixing Layer," *Experimental Thermal and Fluid Science*, Vol. 11, 1995, pp. 210–222.

[13]Maniam, B. M., and Hollingsworth, D. K., "Experimental Investigation of Heat Transfer in a Three-Dimensional Boundary Layer Beneath a Mixing Layer," *Proceedings of the 7th AIAA/ASME Joint Thermophysics and Heat Transfer Conference*, Vol. 2, AIAA, Reston, VA, 1998, pp. 123–130.

[14]Thole, K. A., "High Free-Stream Turbulence Effects on the Transport of Heat and Momentum," Ph.D. Dissertation, Mechanical Engineering Dept., Univ. of Texas, Austin, TX, 1992.

[15]Thole, K. A., and Bogard, D. G., "Enhanced Heat Transfer and Shear Stress due to High Free-Stream Turbulence," *Journal of Turbomachinery*, Vol. 117, 1995, pp. 418–424.

[16]Thole, K. A., and Bogard, D. G., "High Freestream Turbulence Effects on Turbulent Boundary Layers," *Journal of Fluids Engineering*, Vol. 118, 1996, pp. 276–284.

[17]Maciejewski, P. K., and Moffat, R. J., "Heat Transfer with Very High Free-Stream Turbulence, Part I: Experimental Data," *Journal of Heat Transfer*, Vol. 114, 1992, pp. 827–833.

[18]Maciejewski, P. K., and Moffat, R. J., "Heat Transfer with Very High Free-Stream Turbulence, Part II: Analysis," *Journal of Heat Transfer*, Vol. 114, 1992, pp. 834–839.

[19]Bott, D. M., and Bradshaw, P., "Effect of High Levels of Free-Stream Turbulence on Boundary Layer Skin Friction and Heat Transfer," Mechanical Engineering Dept., Rept. MD-75, Stanford Univ., Stanford, CA, 1997.

[20]Bott, D. M., and Bradshaw, P., "Effect of High Free-Stream Turbulence on Boundary Layer Skin Friction and Heat Transfer," AIAA Paper 98-0531, 1998.

[21]Camp, T. R., and Shin, H.-W., "Turbulence Intensity and Length Scale Measurements in Multistage Compressors," *Journal of Turbomachinery*, Vol. 117, 1995, pp. 38–46.

[22] Ames, F. E., and Plesniak, M. W., "The Influence of Large Scale, High Intensity Turbulence on Vane Aerodynamic Losses, Wake Growth, and the Exit Turbulence Parameters," American Society of Mechanical Engineers, ASME Paper 95-GT-290, 1995.

[23] Ames, F. E., "The Influence of Large-Scale High-Intensity Turbulence on Vane Heat Transfer," *Journal of Turbomachinery*, Vol. 119, 1997, pp. 23–30.

[24] Halstead, D. E., Wisler, D. C., Okiishi, T. H., Walker, G. J., Hodson, H. P., and Shin, H.-W., "Boundary Layer Development in Axial Compressors and Turbines: Part 3 of 4—LP Turbines," *Journal of Turbomachinery*, Vol. 119, 1997, pp. 225–237.

[25] Fingerson, L. M., and Freymuth, P., "Thermal Anemometers," *Fluid Mechanics Measurements*, 2nd ed., edited by R. J. Goldstein, Taylor and Francis, Washington, DC, 1996, p. 131.

[26] Maniam, B. M., "An Experimental Study of the Turbulent Momentum and Thermal Boundary Layers Beneath a Two-Stream Mixing Layer," Ph.D. Dissertation, Dept. of Mechanical Engineering, Univ. of Houston, Houston, TX, 1997.

[27] Barrett, M. J., and Hollingsworth, D. K., "Heat Transfer in Turbulent Boundary Layers Subjected to Free-Stream Turbulence—Part I: Experimental Results," *Journal of Turbomachinery*, Vol. 125, 2003, pp. 232–241.

[28] Barrett, M. J., and Hollingsworth, D. K., "On the Calculation of Length Scales for Turbulent Heat Transfer Correlation," *Journal of Heat Transfer*, Vol. 123, 2001, pp. 878–883.

[29] Barrett, M. J., "Skin Friction and Heat Transfer in Turbulent Boundary Layers Subjected to Small-Scale Free-Stream Turbulence," Ph.D. Dissertation, Dept. of Mechanical Engineering, Univ. of Houston, Houston, TX, 1998.

[30] Barrett, M. J., and Hollingsworth, D. K., "On the Correlation of Heat Transfer in Turbulent Boundary Layers Subjected to Free-Stream Turbulence," American Society of Mechanical Engineers, ASME Paper HTD99-76, 1999.

[31] Kays, W. M., and Crawford, M. E., *Convective Heat Transfer*, McGraw–Hill, 1980.

[32] Spalart, P. R., "Direct Simulation of a Turbulent Boundary Layer up to $R_\theta = 1410$," *Journal of Fluid Mechanics*, Vol. 187, 1988, pp. 61–98.

[33] Barrett, M. J., and Hollingsworth, D. K., "Heat Transfer in Turbulent Boundary Layers Subjected to Free-Stream Turbulence—Part II: Analysis and Correlation," *Journal of Turbomachinery*, Vol. 125, 2003, pp. 242–251.

[34] Fernholz, H. H., and Finley, P. J., "The Incompressible Zero-Pressure-Gradient Turbulent Boundary Layer: An Assessment of the Data," *Progress in Aerospace Sciences*, Vol. 32, 1996, pp. 245–311.

R. M. C. So
Associate Editor